Carbon Hybridization to Tight-Binding to Dirac Solid

The Wonder Laboratory of Graphene*

Sushanta Dattagupta

We make a pedagogical survey on why the charge carriers (electrons) in graphene are called massless Dirac fermions. Our analysis begins at the beginning, namely, we start from the quantum chemistry of two nearby carbon (C) atoms and show how their hybridized orbitals 'valence-bond' with each other to form an energy-band in the solid-state. This yields a two-dimensional honeycomb lattice of graphene, which can be viewed as two inter-penetrating triangular sublattices. That recognition provides a perfect setting for describing the dynamics of the last weakly-localized valence electron of C in a tight-binding model, which captures all the unusual electronic phenomena of graphene. The latter emerges from a resemblance to the relativistic Dirac theory of electrons because, in the long-wavelength limit, the energy dispersion is linear in the wave vector. We build up – step by step – this remarkable transition of a carbon-based material to an exotic two-dimensional Dirac solid, in which much of the quantum aspects of modern condensed matte physics can be tested in the laboratory.

Sushanta Dattagupta, having spent more than forty years in teaching, research and administration in various institutions and universities across India, is now a senior scientist of the Indian National Science Academy. He has written extensively, in journals and books, on topics of condensed matter, non-equilibrium phenomena, and more recently Tagore Model of education. His current physics interests are in quantum dissipation and stochastic thermodynamics of nanoscopic systems.

Keywords
Graphene, hybrid orbitals, tight-binding, pseudo-spin, massless fermions, Dirac theory.

1. Introduction

The purpose of this 'General Article' is to present in simple terms – accessible to university students of chemistry and physics – the underlying ideas behind the epithet of 'Dirac Solid' being attributed to graphene [1–3]. Normally, the Dirac equation, which marries quantum mechanics with the special theory of relativity, is relevant to particles that move with nearly the speed of light c. Why then electrons, which in a semimetal like graphene, travel

*Vol.25, No.2, DOI: https://doi.org/10.1007/s12045-020-0939-5

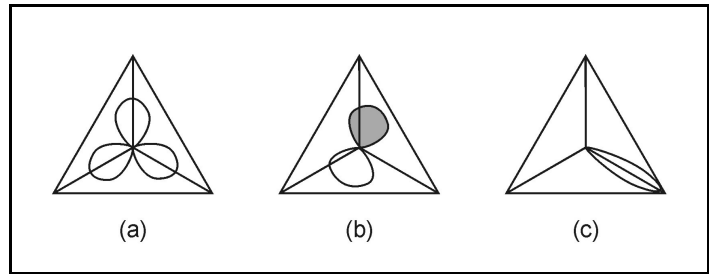

Figure 1. **(a)** Three hybrid orbitals at an angle of 120° with each other. **(b)** The unhybridized p_z orbitals normal to the X-Y planbe. **(c)** Covalent bond between two C-atoms.

Why then electrons, which in a semimetal like graphene, travel with a speed that is estimated to be one-three hundredth of c, are believed to have properties akin to Dirac fermions?

with a speed that is estimated to be one-three hundredth of c, are believed to have properties akin to Dirac fermions? Further, why are these fermions endowed with zero mass, which immediately lend them a property, called chirality (handedness)? The latter is associated with helicity that is linked in the Dirac theory of relativistic electrons with the intrinsic electron-spin. But, in graphene, the spin is actually a pseudo-spin; what is its physical meaning? We attempt to answer all these questions which students with background in quantum theory and solid state chemistry/physics ought to be able to follow.

Graphene, the one-atom thick two-dimensional sheet of graphite, is an allotrope of carbon (C). It has caused sensation in the world of chemistry and physics of solids [4, 5]. The excitement hinges on its exotic electronic and mechanical properties. It is because of their immense technological uses, various allotropes of carbon, such as fullerene (a zero-dimensional molecule of 60 or 70 C atoms) and the two-dimensional graphene which can be rolled into three-dimensional C nanotubes [6], have attracted two Nobel prizes – to Kroto, Curl and Smalley for fullerene (1996) [7] and to Geim and Novoselov for graphene (2010) [8]. We will therefore construct the story of graphene, from the 'bottom-up', namely how the electronic orbitals of C atoms bond together to form a two-dimensional honeycomb structure of graphene (*Figure* 2, in Section 2). In graphene, both the intra-layer atomic spacing ~ 0.14 nm and the four-time bigger inter-layer distance are in the nm-range, hence graphene is an epitome of a nano material.

In graphene, both the intra-layer atomic spacing ~ 0.14 nm and the four-time bigger inter-layer distance are in the nm-range, hence grapheme is an epitome of a nano material.

The C-hybridization leads to σ-bonded valence electrons stabi-

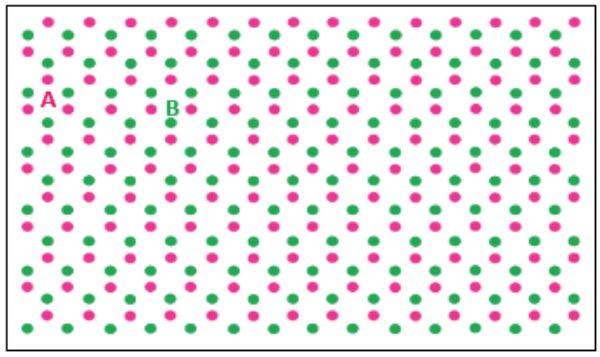

Figure 2. Honeycomb lattice formed by carbon atoms in graphene.

lizing into a planar honeycomb lattice. On the other hand, somewhat weakly localized π-electrons can hop (i.e., tunnel) from one lattice site to a nearest neighbour (nn) site, thus yielding a tight-binding (TB) model, familiar in solid state physics. This issue will be discussed in detail in Section 3. The special lattice structure however gives rise, in the reciprocal momentum-space, to a dispersion relation (between energy E and wave vector **k**) or a band structure. The remarkable aspect of this dispersion in graphene is that the energy E turns out to be a 2×2 matrix, much like a Dirac spinor in which the two basis states of the matrix represent the two spin-states of the electron. However, in graphene, the two states correspond to the occupation of the two nn-sites of the inter-penetrating triangular sublattices that the honey comb structure subsumes and are therefore, the eigenstates of not a real spin but a *pseudo-spin*.

In graphene, the two states correspond to the occupation of the two nn-sites of the inter-penetrating triangular sublattices that the honey comb structure subsumes and are therefore, the eigenstates of not a real spin but a *pseudo-spin*.

Once the TB model is set up in the reciprocal space, it is straightforward to see that very near the so-called K and K′ points that are symmetrically situated at the two corners of the graphene Brillouin zone (*Figure* 4, in Section 3), the dispersion relation is linear in $|\mathbf{k}|$, say near the K-point [1,2]. This is analogous to the energy-momentum relation for fermions that travel with the speed of light. It is this analogy that prompts the coinage: 'Dirac fermion' for the de-localized electrons in graphene. But, so far, we only have a spinor representing the pseudo-spin; where is the 4×4 Γ-matrix description of the full Dirac theory, discussed in

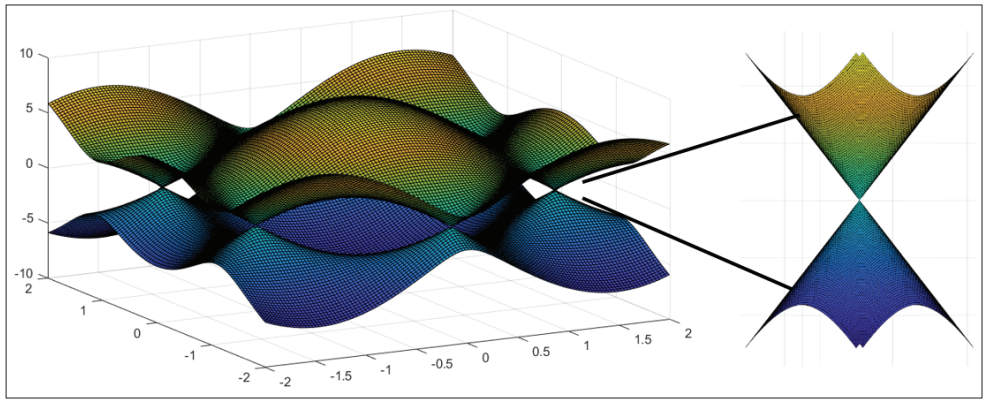

Figure 3. **(a)** Electronic energy dispersion of honeycomb lattice of graphene. **(b)** Zoom view of single Dirac point of energy bands.

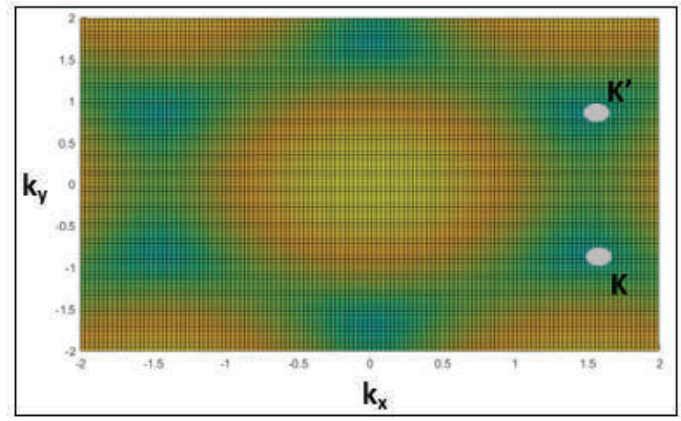

Figure 4. Top view of electronic energy dispersion of graphene shown in *Figure* 3(a).

Section 4 below, coming from? To see this unfold we have to bring-in the K′-point as well into reckoning and employ the so-called Weyl representation of the Dirac equation [3]. All that will be expanded upon, in Section 5 below.

It is not for the first time that graphene is being attempted to feature as a regular article in *Resonance*. Because of the extraordinary status of it being the material for the future, there have been two previous pieces on graphene. Desmukh and Singh had, in 2011, dwelt on the technological aspects – especially, the 'Scotch-tape' technique of preparation, and applications ensuing from unique electronic and mechanical properties of graphene

[9]. Potnis, on the other hand, in a more recent *Resonance* article in 2017, had focused on the various allotropes of C, e.g., C-nanotube, fullerene, Bucky paper (macroscopic aggregate of C nanotubes) and of course, graphene, as well [10]. The emphasis has been on numerous applications of these C-based materials. Our aim, however, is a complementary one – to elucidate on the basic quantum theoretical aspects of graphene and to point out how some unusual consequences of Dirac physics – that are often beyond the reach of laboratory particle physics – can be brought down to the realm of the solid state.

2. Carbon Hybridization

A free C atom has 6 electrons. Two of these are strongly bound core electrons in the quantum state designated as 1s, wherein the orbital quantum number I = 0 (s-state), and the principal quantum number n = 1. These core electrons need no further deliberation as they are so deep inside that they have no consequence for solid state properties. That leaves us with 4 electrons, called valence electrons, that have to be accommodated in the n = 2 orbitals. Two of these enter and fill the 2s orbital (in opposite spin configuration in accordance with the Pauli principle) leaving a pair to fill-in the 2p subshell. Thus the ground state configuration of C may be written as $1s^2 2s^2 2p^2$. There is a catch though [11]. Because of Coulomb repulsion we expect the other two electrons to occupy not the same but two different 2p orbitals. Thus we can assign one electron to the $2p_x$ orbital and the other to the $2p_y$ orbital. Although the x, y and z directions are arbitrarily chosen we may employ the above-mentioned XY-plane as the one that will eventually define the graphene layer. Thus, the lowest energy configuration can be denoted as $1s^2 2s^2 2p_x{}^1 2p_y{}^1$. Because of Hund's rule the two 2p electrons have the same spin and hence, are unpaired. There is now another caveat – the presence of just two unpaired electrons in the 2p orbitals would lead to only two bonds when say, two different C atoms or a C atom and another distinct atom, are brought near. But, in point of fact, C is tetravalent, like in methane (CH_4)! This issue is resolved by allowing

The further mixing of one 2s and two 2p atomic orbitals (p_x and p_y, in this case) is called *hybridization*.

for 'promotion' – the excitation of an electron from the $2s^2$ orbital to a vacant 2p orbital, namely $2p_z$ [11]. At first sight, promotion may appear to cost excess energy but that is more than offset by the relief provided on account of the Coulomb repulsion among the two 2s electrons. Taking all these points into account we arrive at the following valence state configuration for a C atom: $2s^1 2p_s^1 2p_y^1 2p_z^1$, with *four* unpaired electrons in separate orbitals. The further mixing of one 2s and two 2p atomic orbitals (p_x and p_y, in this case) is called *hybridization*. When it comes to graphene the fourth unpaired, unhybridized electron goes to the (*half-filled*) $2p_z$ orbital which lies perpendicular to its plane (viz., XY).

While a C atom can, in general, admit three possible kinds of hybridization (sp, sp^2, sp^3 – not to be confused with our earlier spectroscopic notation) the one that is applicable to graphene is known as sp^2 hybridization which we explain now. A sp^2 hybrid is a superposed wavefunction of one 2s orbital and two 2p ($2p_x$ and $2p_y$) orbitals that can take one of the three following forms [6, 11]:

$$|sp^2_a\rangle = (|2s\rangle - \sqrt{2}|2p_y\rangle)/\sqrt{3},\ |sp^2_{b(c)}\rangle = (+(-1)|2s\rangle + 1/\sqrt{2}[\sqrt{3}|2p_x\rangle + (-)|2p_y\rangle])/\sqrt{3}\,. \quad (1)$$

Because Eq.(1) entails the mixing of an s orbital with two p orbitals the above is referred to as sp^2 hybridization. As shown in *Figure* 1(a) the three hybrid orbitals in Eq. (1) lie in a plane and point towards the corners of an equilateral triangle. As mentioned earlier, the $2p_z$ orbital is not included in the hybridization and its axis is normal to the XY-plane in which the hybrids lie (*Figure* 1 (b)). As it turns out, it is this weakest bound electron that is responsible for all spectacular properties of graphene.

We will now like to graduate from a single C atom to say, a pair of C atoms. It was the physical chemist G. N. Lewis – an *unsung hero* – who first discussed the notion of a *covalent bond* between two atoms (in 1916, even before quantum mechanics was fully

unravelled [12]). The resulting *valence-bond* theory describes each electron pair in neighbouring atoms by a wave function that accommodates either member of the pair to be simultaneously found on both atoms, joined by the bond. As we discussed in the preceding paragraph, the sp^2 hybrids in C fan out in three different directions at an angle of 120^o with each other (*Figure* 1 (a)). Thus each of these orbitals (designated by the subscript a, b or c, in Eq. (1)) can find its twin brother in a neighbouring C atom and form a covalent bond (*Figure* 1 (c)). This, in the valence-bond theory, is called *a-bond*. The symbol σ (which is Greek s) has its origin in the fact that the sp^2 hybrids in *Figures* 1 (a) and 1 (c) have planar or cylindrical symmetry with respect to the Z-axis. Since both the position and momentum vectors of electrons belonging to the sp^2 orbital lie in the XY-plane, the angular momentum about the Z-axis is zero, and hence, when viewed along this axis, they exhibit s-wave-like symmetry! It is indeed fascinating to realize that it is the 120^o orientations of the three (strongly) σ-bonded pairs of neighbouring C atoms which yield the honeycomb structure of planar graphene in which each C atom finds itself three nn-C atoms at the vertices, indicated by pink and green alternately, of an equilateral triangle (*Figure* 2). Once the structure is in place it is the lone $2p_z$ electron of a C atom that can bind with a similar $2p_z$ electron of a nearby C atom. Because this kind of bonding results from electrons in two p orbitals that approach each other side-by-side – and when, viewed along the Z-axis, resembles a pair of electrons in a p orbital – it is called a π-bond (as π is the Greek equivalent of p). Again, Hund's rule suggests that the two electrons belonging to the π-bond have the same spin. Therefore, in the TB- picture (discussed below) in which the π-bond implies entanglement of two electrons in the nn-sublattice sites (*Figure* 2), the electron spin is of no consequence.

The resulting *valence-bond* theory describes each electron pair in neighbouring atoms by a wave function that accommodates either member of the pair to be simultaneously found on both atoms, joined by the bond.

3. Tight-Binding (TB) Model

Given this background laid out in Section. 2, we now focus on the hexagonal structure of graphene, introduced earlier in *Figure* 2 and its reciprocal lattice. What is shown in *Figure* 2 is not a

Bravais lattice [13] but two interpenetrating lattices of equilateral triangles. These two sublattices are denoted by the symbols A (say, pink) and B (say, green). An electron at an A-site can *jump* to a B-site, with allowance for only nn *hops*. The phrases: *jumps* and *hops* are only loosely expressed here – in quantum mechanical terms, there is overlap of the wave function of the electron between the A and B-sites. A delocalized electron is neither at an A-site nor at a B-site – it is in a mixed superposed state. If the electron is at an i^{th} A-site we designate that quantum state by the Dirac ket [14] : $|+\rangle_{i\{A\}}$; on the other hand, an unoccupied state or a hole is denoted as: $|-\rangle_{i\{A\}}$. The $|+\rangle$ and $|-\rangle$ are taken to represent the basis states of the third component of a pseudo-spin σ_3

$$\sigma_3 = \begin{pmatrix} 1 & 0 \\ 0 & -1 \end{pmatrix}, |+\rangle = \begin{pmatrix} 1 \\ 0 \end{pmatrix}, |-\rangle = \begin{pmatrix} 0 \\ 1 \end{pmatrix}. \tag{2}$$

The mixed states are the symmetric and anti-symmetric combinations akin to the bonding and anti-bonding states of Pauling [15]:

$$|S\rangle = \left(\frac{1}{\sqrt{2}}\right)[|+\rangle + |-\rangle],$$
$$|A\rangle = \left(\frac{1}{\sqrt{2}}\right)[|+\rangle - |-\rangle]. \tag{3}$$

The two π electrons in nn-sites of graphene can belong to either the bonding or the anti-bonding state or an admixture of both. In a tutorial discourse on the tight-binding model it was argued in [16] that the bonding state leads to stronger binding than the anti-bonding state, because of the finiteness of the electron probability density in the middle of two C nuclei in view of higher Coulomb attraction. Following the same arguments as given in [16], we are led to the TB model, which in the present case, is described by the Hamiltonian:

$$H = -t\,\Sigma_{\langle i\{A\}j\{B\}\rangle}\,(|+\rangle_{i\{A\}}\langle -|_{j\{B\}} + |-\rangle_{j\{B\}}\langle +|_{i\{A\}}) \tag{4}$$

where t is the so-called hopping integral also known as the tunnel-splitting. As stressed earlier the actual electron spin does not enter

into H and is therefore, not indicated here. Keeping in view the translational invariance of the two-dimensional graphene lattice we may rewrite H by going to the Bloch-Fourier space:

$$|+\rangle_{i\{A\}} = \Sigma_k |+\ \mathbf{k}\rangle \exp(i\mathbf{k}.\mathbf{R}_i),$$
$$\langle -|_j\{B\} = \Sigma'_{\mathbf{k}} \langle -, \mathbf{k}'| \exp(-i\mathbf{k}'.R_j) \quad (5)$$

Introducing the nn-vector δ as [2]

$$\mathbf{R}_i = \mathbf{R}_i + \delta \quad (6)$$

we obtain from Eq. (4),

$$H = -\Sigma_{\mathbf{k}}(t(\mathbf{k})|+,\mathbf{k}\rangle\langle -,\mathbf{k}| + t^*(\mathbf{k})\,|-,\mathbf{k}\rangle\langle +,\mathbf{k}|), \quad (7)$$

where

$$t(\mathbf{k}) = 2\pi\, t\, \Sigma_\delta \exp(-i\,\mathbf{k}.\,\delta) \quad (8)$$

In arriving at Eq. (8) we have employed periodic boundary conditions of the two-dimensional lattice which yield

$$\Sigma_i \exp(i(\mathbf{k}-\mathbf{k}').\mathbf{R}_i) = \mathbf{2}\pi\delta(\mathbf{k}-\mathbf{k}') \quad (9)$$

For a fixed $\mathbf{k}$, H can be written as a 2×2 matrix with rows and columns labelled by $|+,\mathbf{k}\rangle$ and $|-,\mathbf{k}\rangle$:

$$H_{\mathbf{k}} = \begin{pmatrix} 0 & -t(\mathbf{k}) \\ -t^*(\mathbf{k}) & 0 \end{pmatrix}. \quad (10)$$

We have now fulfilled our first promise – the Hamiltonian in the k-space is indeed a spinor but in the pseudo-spin states! To see this more explicitly we may rewrite Eq. (10) in terms of the first two components of Pauli spin operator:

$$H_{\mathbf{k}} = -\mathrm{Re}\, t(\mathbf{k})\,\sigma_1 + \mathrm{Im}\, t(\mathbf{k})\sigma_2, \quad (11)$$

where

$$\sigma_1 = \begin{pmatrix} 0 & 1 \\ 1 & 0 \end{pmatrix} \quad \text{and} \quad \sigma_2 = \begin{pmatrix} 0 & -i \\ i & 0 \end{pmatrix} \quad (12)$$

It is easy to diagonalize the matrix in Eq. (10) yielding the eigenvalues:

$$\epsilon_{\mathbf{k}} = \sqrt{|t(\mathbf{k})|^2} \ \text{ or } -\sqrt{|t(\mathbf{k})^2}. \quad (13)$$

Thus, the energy has two branches – positive (for electrons) and negative (for holes), similar to electron-positron (particle-anti-particle) picture of Dirac (see Sec. 4 below), and defining in the present case, the conduction and valence bands respectively (*Figure* 3). In the absolute ground state the valence band is completely filled while the conduction band is completely unoccupied, reflecting the half-filled nature of the p_z orbital, to begin with.It is the electrons that are thermally promoted from the valence to the conduction band which define the physical properties of graphene. The behaviour of $\epsilon_{\mathbf{k}}$ vs. k is what is known as the dispersion relation. In order to comprehend this, we have to construct the Brillouin zone in the reciprocal space [13]. The dispersion relation gives rise to a band structure which is graphically exhibited in the Resonance article of [9]. As shown there, the conduction and valence bands symmetrically located above and below the Fermi level, touch each other at 6 points where the band gap is zero (*Figure* 3 (a)). These six Fermi points, indicated by dark circles in *Figure* 4, again have hexagonal symmetry. Only two of these, marked by K and K′ are special points, the others being mirror images. An electron can belong to either the K- or the K′-valley, just as it can have two spin-projections 'up' and 'down', and it is this two-state attribute that is sometime in the literature given the nomenclature of a 'pseudo-spin'[9]. However, we prefer to represent the presence (electron) or absence (hole) of a particle in the real space of grapheme lattice by a pseudo-spin, as indicated earlier in Eq. (2).

We are now ready, with reference to *Figures* 2–4, to provide the details of the lattice parameters, in real and reciprocal spaces. The lattice vectors defining one of the equilateral triangles in *Figure* 2, are given by

$$\mathbf{a}_1 = \frac{a}{2}(3,\ \sqrt{3}), \mathbf{a}_2 = \frac{a}{2}(3, -\sqrt{3}). \tag{14}$$

where a $\sim$ 0.14 nm is the C-C distance.The three nn vectors are:

$$\delta_1 = \frac{a}{2}(1,\ \sqrt{3}), \delta_2 = \frac{a}{2}(1, -\sqrt{3}), \delta_3 = a(-1, 0). \tag{15}$$

The reciprocal-lattice vectors can be written as

$$\mathbf{b} = \frac{2\pi}{3a}(1,\ \sqrt{3}), \mathbf{b}_2 = \frac{2\pi}{3a}(1, -\sqrt{3}), \tag{16}$$

clearly satisfying

$$\mathbf{a}_{\mathrm{m}}.\mathbf{b}_{\mathrm{n}} = 2\pi\ \delta_{\mathrm{mn}} \tag{17}$$

The K and the K′ points (*Figure* 4) are defined by

$$\mathbf{K} = \frac{2\pi}{3\mathrm{a}}\left(1, \frac{1}{\sqrt{3}}\right), \mathbf{K}' = \frac{2\pi}{3\mathrm{a}}\left(1, \frac{-1}{\sqrt{3}}\right). \tag{18}$$

From Eq. (8),

$$\mathrm{t}_{\mathbf{K}}(\mathbf{q}) = -\left(\frac{3\pi\mathrm{ta}}{2}\right)(\mathrm{i} + \sqrt{3})(\mathrm{q}_{\mathrm{x}} - \mathrm{iq}_{\mathrm{y}}) = -\hbar\,\mathrm{v}\,|\mathbf{q}|\exp\left[i\left(\pi/6 - \theta_q\right)\right], \tag{19}$$

where the subscript K implies that in evaluating the tunnelling energy t (**q**) we have focused on the region near the **K**-point in the Brillouin zone, written **k = K + q**, and made an expansion around **K** to linear order in **q**, keeping in view Eq. (20); the parameter v (= $3\pi ta/\hbar$) has the dimension of a velocity which is (somewhat loosely) called the Fermi velocity. The point is, the Fermi energy is quadratic in the Fermi velocity, unlike in the linear relation depicted in Eq. (19). The question arises: why expand to linear order in the wave vector? The reason is, at low temperatures wherein quantum effects are significant, only states near K = 0 (or K′ = 0) are relevant as far as thermodynamic and transport properties are concerned. (The situation is similar to the one concerning the low-temperature heat capacity of a metal wherein only the electron-hole excitations near the Fermi level matter [13].)

From Eq. (10), the Hamiltonian near the **K**-point can be written as

$$\mathrm{H}_{\mathrm{K}}(\mathbf{q}) = \hbar v|\mathbf{q}|\begin{pmatrix} 0 & \exp - i\left(\frac{\pi}{6} - \theta\mathbf{q}\right) \\ \exp[-i\left(\frac{\pi}{6} - \theta_{\mathbf{q}}\right) & 0 \end{pmatrix} \tag{20}$$

It is evident that the two eigenvalues are

$$\lambda_{\mathbf{K}}(\mathbf{q}) = +\hbar\mathrm{v}|\mathbf{q}| \ \text{ and } -\hbar\mathrm{v}|\mathbf{q}|, \tag{21}$$

with the corresponding eigenfunctions

$$\psi_{+\mathbf{K}}(\mathbf{q}) = \frac{1}{\sqrt{2}}\begin{pmatrix}\exp(\frac{i}{2}\left[\frac{\pi}{6} - \theta\mathbf{q}\right]\\ \exp(\frac{-i}{2}\left[\frac{\pi}{6} - \theta\mathbf{q}\right]\end{pmatrix} \text{ and}$$

$$\psi_{-\mathbf{K}}(\mathbf{q}) = \frac{1}{\sqrt{2}}\begin{pmatrix}\exp(\frac{i}{2}\left[\frac{\pi}{6} - \theta\mathbf{q}\right]\\ \exp(\frac{-i}{2}\left[\frac{\pi}{6} - \theta\mathbf{q}\right]\end{pmatrix} \tag{22}$$

where $\psi_{+\mathbf{K}}$ $(\mathbf{q})$ is assigned to the **conduction band** and $\psi_{-\mathbf{K}}$ $(\mathbf{q})$ to the **valence band**. It is a bit cumbersome to carry the constant phase factor of exp (i $\pi/6$) in Eq. (19). It can be easily eliminated by rotating the vector $\mathbf{q}$ about the Z-axis by an angle $\pi/6$ in the clockwise direction yielding a new wave vector $\mathbf{q}$ whose components are

$$\begin{aligned} \mathrm{q_{x'}} &= \frac{(\sqrt{3}\mathrm{q_x} + \mathrm{q_v})}{2}, \\ \mathrm{q_{y'}} &= \frac{(-\mathrm{q_x} + \sqrt{3}\,\mathrm{q_v})}{2}. \end{aligned} \tag{23}$$

Evidently, from Eq. (19),

$$\mathbf{t_K}(\mathbf{q}') = -\hbar\mathrm{v}(q'_x - iq'_y),$$

which, upon re-denoting $\mathbf{q}$ as $\mathbf{q}'$, yields

$$\mathbf{t_K}(\mathbf{q}) = -\hbar\mathrm{v}\,(\mathrm{q_x} - \mathrm{i}\,\mathrm{q_y}). \tag{24}$$

Consequently, in this new representation of the wave vector the constant phase can be dropped for further consideration from Eq. (22), or in more fancy language, the phase can be 'gauged away'. Further, from Eq. (2), we note that the eigenfunctions can be expressed as a linear superposition of the basis states $|+\rangle$ and $|-\rangle$:

$$\psi_{\mathbf{K}}(\mathbf{q}) = \left[\exp\left(-i\frac{\theta_\mathrm{q}}{2}\right)|+\rangle + \exp\left(i\frac{\theta_\mathrm{q}}{2}\right)|-\rangle\right] / \sqrt{2} \tag{25}$$

Similarly,

$$\psi_{\mathbf{K}}(\mathbf{q}) = \left[\exp\left(-i\frac{\theta_\mathrm{q}}{2}\right)|+\rangle - \exp\left(i\frac{\theta_\mathrm{q}}{2}\right)|-\rangle\right] / \sqrt{2} \tag{26}$$

Thus, as already stated in the beginning of this section, the electron in the conduction band (described by Eq. (25)) or the valence band (described by Eq. (26)) is neither in the A-sublattice site or the B-sublattice site but is in a coherent superposed state in-between!Finally, combining Eq. (10) with Eq. (24) and employing the definition of the Pauli matrices as in Eq. (12), we can express the Hamiltonian in the compact form:

$$H_{\mathbf{K}}(\mathbf{q}) = \hbar \mathrm{v}\,(\sigma.\mathbf{q})\,. \tag{27}$$

where σ is a two-dimensional vector-operator.

We now turn our attention to the $\mathbf{K}'$ point (*Figure* 4) which is obtained from the $\mathbf{K}$-point by replacing $\mathrm{k_y}$ by $-\mathrm{k_y}$, which is tantamount to taking the complex conjugate of Eq. (24). Hence, in parallel to Eq. (27) we can write

$$H_{\mathbf{K}'}(\mathbf{q}) = \hbar \mathrm{v}\,(\sigma^*.\mathbf{q})\,. \tag{28}$$

where the two components of σ^* are obtained by taking the complex conjugate of Eq. (12).The full Hamiltonian then has the following 4×4 matrix representations:

$$H(\mathbf{q}) = \hbar \mathrm{v} \begin{pmatrix} \sigma.\mathbf{q} & 0 \\ 0 & \sigma^*.\mathbf{q} \end{pmatrix} \tag{29}$$

wherein the upper left 2×2 block refers to the K-valley whereas the lower right 2×2 block refers to the K′ valley.

4. Dirac Theory of Relativistic Electrons – A Summary

Following the astonishing development of Quantum Mechanics in the 1920's the Dirac equation (1928) was a further significant step in successfully integrating quantum theory with the special theory of relativity [17]. Recall that for particles moving with relativistic speeds (v˜c, the speed of light) the energy E – rest mass m – momentum p relation reads

$$\mathrm{E}^2 = \mathrm{m}^2\mathrm{c}^4 + \mathrm{p}^2\mathrm{c}^2. \tag{30}$$

For non-relativistic speeds ($v \ll c$), the rest mass term dominates:

$$E^2 = m^2c^4, E = +mc^2 \text{or} - mc^2. \tag{31}$$

On the other hand, for ultra relativistic speeds,

$$E^2 \sim p^2c^2, E \sim |p|c \text{or} - |p|c. \tag{32}$$

Quite remarkably, the energy is now linear in the momentum in contrast to non-relativistic mechanics in which the energy is quadratic in p. Recall that the non-relativistic Schrödinger equation of quantum mechanics is first order in time and second order in space, and is therefore at variance with the special theory. The genius of Dirac, purely inspired by mathematical elegance of symmetry, led him to write the now-famous equation – first order in both space and time [18]:

$$i\left(\frac{\partial}{\partial t}\right)\psi(\mathbf{r}, t) = \left(-i\, c\, \boldsymbol{\alpha}.\nabla + \beta\,(mc^2/\hbar)\right)\psi(\mathbf{r}, t) \tag{33}$$

In order to incorporate the intrinsic electronic spin the wave function $\psi(\mathbf{r}, t)$ must be a two-component spinor, to start with. In addition, the energy-momentum relation in Eq. (30) admits two branches, for positive energy and negative energy, corresponding to a particle and its anti-particle. When it comes to an electron the anti particle is a positron (discovered, incidentally, four years after Dirac predicted it purely from theoretical considerations!). Therefore, ψ ($\mathbf{r}$, t) has to be a four-component spinor the components of which can be written, separately in the electron and positron sectors, as

$$\psi^e \uparrow (\mathbf{r}, t) = |e \uparrow (\mathbf{r}, t)\rangle, \psi^e \downarrow (\mathbf{r}, t)\rangle = |e \downarrow (\mathbf{r}, t)\rangle, \psi^\pi \uparrow (\mathbf{r}, t) =$$

$$|\pi \uparrow (\mathbf{r}, t)\rangle, \psi^n \downarrow (\mathbf{r}, t) = |\pi \downarrow (\mathbf{r}, t)\rangle \tag{34}$$

where the arrows up and down represent the two spin states, and π denotes the positron. Evidently, simultaneous charge-conjugation and time-reversal would make $\psi^e \uparrow (\mathbf{r}, t)$ go into $\psi^n \downarrow (\mathbf{r}, t)$ and $\psi^e \downarrow (\mathbf{r}, t)$ into $\psi^n \uparrow (\mathbf{r}, t)$. Correspondingly each Cartesian component of the vector operator σ and the scalar operator β is a four-component matrix with the following representations

$$\alpha = \begin{pmatrix} \mathbf{0} & \boldsymbol{\sigma} \\ \boldsymbol{\sigma} & \mathbf{0} \end{pmatrix}, \quad \beta = \begin{pmatrix} \mathbf{I} & \mathbf{0} \\ \mathbf{0} & -\mathbf{I} \end{pmatrix}. \tag{35}$$

where the three components of σ have been introduced earlier (cf., Eqs. (2) and (12)), and **1** is the unit matrix. The Hamiltonian matrix, associated with Eq. (31) has the representation:

$$\mathrm{H} = \begin{pmatrix} \mathbf{I}.\mathrm{mc2} & c\boldsymbol{\sigma}.\mathbf{p} \\ \mathbf{c}\boldsymbol{\sigma}.\mathbf{p} & -\mathbf{I}.mc2 \end{pmatrix}. \tag{36}$$

In component form Eq. (33) can be expanded as

$$(i\hbar)\frac{\partial}{\partial t}|e\uparrow(\mathbf{r},\mathbf{t})\rangle = \mathrm{mc}^2|\mathrm{e}\uparrow(\mathbf{r},\mathbf{t})\rangle+\mathrm{cp_z}|\pi\uparrow(\mathbf{r},\mathbf{t})\rangle+\mathrm{c}(\mathrm{p_x}-\mathrm{ip_y})|\pi\downarrow(\mathbf{r},\mathbf{t})\rangle \tag{37a}$$

$$(i\hbar)\frac{\partial}{\partial t}|e\downarrow(\mathbf{r},\mathbf{t})\rangle = \mathrm{mc}^2|\mathrm{e}\downarrow(\mathbf{r},\mathbf{t})\rangle-\mathrm{cp_z}|\pi\downarrow(\mathbf{r},\mathbf{t})\rangle+\mathrm{c}(\mathrm{p_x}+\mathrm{ip_y})|\pi\uparrow(\mathbf{r},\mathbf{t})\rangle\,, \tag{37b}$$

$$(i\hbar)\frac{\partial}{\partial t}|\pi\uparrow(\mathbf{r},\mathbf{t})\rangle = -\mathrm{mc}^2|\pi\uparrow(\mathbf{r},\mathbf{t})\rangle+\mathrm{cp_z}|\mathrm{e}\uparrow(\mathbf{r},\mathbf{t})\rangle+\mathrm{c}(\mathrm{p_x}-\mathrm{ip_y})|\mathrm{e}\downarrow(\mathbf{r},\mathbf{t})\rangle \tag{37c}$$

$$(i\hbar)\frac{\partial}{\partial t}|\pi\downarrow(\mathbf{r},\mathbf{t}) = -\mathrm{mc}^2|\pi\downarrow(\mathbf{r},\mathbf{t})\rangle - \mathrm{cp_z}|\mathrm{e}\downarrow(\mathbf{r},\mathbf{t})\rangle + \mathrm{c}(\mathrm{p_x}+\mathrm{ip_y})|\mathrm{e}\uparrow(\mathbf{r},\mathbf{t})\rangle \tag{37d}$$

The coupling between the intrinsic spin σ and the momentum **p**, inherent in the Dirac equation, yields the concept of a 'helicity' operator Σ which is defined through

$$(\Sigma.\mathbf{p}) = \begin{pmatrix} \sigma.\mathbf{p} & \mathbf{0} \\ \mathbf{0} & \sigma.\mathbf{p} \end{pmatrix}. \tag{38}$$

a 4/4 matrix that describes the projection of the spin along the direction of motion. Because σ transforms like the orbital angular momentum under coordinate transformation the helicity operator is not invariant under parity transformation. Thus it yields the notion of 'chirality' i.e., left- or right-handedness. Further, the admixture of spin and the orbital part of the wave function (via the different components of the **k**-vector) is an automatic manifestation, in the Dirac theory, of the spin-orbit interaction that is a natural consequence of Maxwellian electrodynamics and the special theory of relativity.

The admixture of spin and the orbital part of the wave function (via the different components of the **k**-vector) is an automatic manifestation, in the Dirac theory, of the spin-orbit interaction that is a natural consequence of Maxwellian electrodynamics and the special theory of relativity.

5. From 3+1 to 2+1 dimension – Transition from Dirac to Graphene Physics

The set of Dirac equations (37) are in 3 space plus 1 time dimensions. They are written in the 2×2 particle (i.e., electron) and 2×2 anti-particle (i.e., positron) sectors. There are however alternate ways of writing these equations, e.g., by grouping the electron (of a particular spin-orientation) with its CT-conjugated positron (in the opposite spin direction), i.e., by pairing Eq. (37a) with Eq. (37d), and Eq. (37b) with Eq. (37c), as indicated following Eq. (34). The resultant Weyl representation, historically introduced to account for zero-mass particles with ultra-relativistic speeds, e.g., neutrino, and additionally in 2 dimensions (such that the Z-motion can be suppressed) is associated with an alternate form of the Hamiltonian than given in Eq. (36)

$$\mathrm{H} = \begin{pmatrix} c\sigma.\mathbf{p} & 0 \\ 0 & c\sigma.\mathbf{p} \end{pmatrix}. \tag{39}$$

With this, the Weyl equations read:

$$(i\hbar)\left(\frac{\partial}{\partial t}\right)|e\uparrow(\mathbf{r},\mathbf{t})\rangle = c(p_x - ip_y)|\pi\downarrow(\mathbf{r},\mathbf{t})\rangle$$

$$(i\hbar)\left(\frac{\partial}{\partial t}\right)|\pi\downarrow(\mathbf{r},\mathbf{t})\rangle = c(p_x + ip_y)|e\uparrow(\mathbf{r},\mathbf{t})\rangle; \tag{40}$$

and

$$(i\hbar)\left(\frac{\partial}{\partial t}\right)|e\downarrow(\mathbf{r},t)\rangle = c(p_x + ip_y)|\pi\uparrow(\mathbf{r},t)\rangle,$$

$$(i\hbar)\left(\frac{\partial}{\partial t}\right)|\pi\uparrow(\mathbf{r},t)\rangle = c(p_x - ip_y)|e\downarrow(\mathbf{r},t)\rangle. \tag{41}$$

Taking Fourier transform the above can be re-written as

$$(i)\left(\frac{\partial}{\partial t}\right)|e\uparrow(\mathbf{q},t)\rangle = c(q_x - iq_y)|\pi\downarrow(\mathbf{q},t)\rangle,$$

$$(i)\left(\frac{\partial}{\partial t}\right)|\pi\downarrow(\mathbf{q},t)\rangle = c(q_x + iq_y)|e\uparrow(\mathbf{q},t)\rangle; \tag{42}$$

and

$$(i)\left(\frac{\partial}{\partial t}\right)|e\downarrow(\mathbf{q},t)\rangle = c(q_x + iq_y)|\pi\uparrow(\mathbf{q},t)\rangle,$$

$$(i)\left(\frac{\partial}{\partial t}\right)|\pi\uparrow(\mathbf{q},t)\rangle = c(q_x - iq_y)|e\downarrow(\mathbf{q},t)\rangle \qquad (43)$$

wherein we have employed the differential form of the momentum operators. On the other hand, if we write the four-component Schroedinger equations appropriate to the graphene Hamiltonian in Eq. (29), wherein the four components are $|+,\mathbf{q}\rangle_{\mathbf{K}}, |-,\mathbf{q}\rangle_K$, $|+,\mathbf{q}\rangle_{K'}$ and $|-,\mathbf{q}\rangle'_K$, quite remarkably, the set of equations for the K-valley are the same in structure as Eq. (42′), while those for the K′-valley are equivalent to Eq. (43′). This identification, which is strictly a mere analogy, also makes it amply clear that zero-mass excitations have nothing to do with the real electron-mass (mind you, the kinetic energy for non-relativistic graphene electrons continues to be quadratic in the momentum), and that v, which has the dimension of velocity, is simply analogous to the speed of light c! It is the (fortuitous) energy-momentum (linear) dispersion which as at the heart of the entire Dirac physics of graphene.

It is the (fortuitous) energy-momentum (linear) dispersion which as at the heart of the entire Dirac physics of graphene.

6. Summary and Concluding Remarks

We first summarize the salient points before presenting our conclusions.

1. Two of the 6 C electrons are core electrons (of no further consequence) while the other 4 are valence electrons.

2. Of the 4 valence electrons 3 are strongly bonded in a hybridized σ orbital while the fourth unpaired electron remains in a half-filled 2p orbital.

3. In the crystallized form of graphene the σ bond yields the honeycomb lattice of hexagonal symmetry with each C atom having three nn C atoms on the vertices of an equilateral triangle.

4. The unpaired electron in the half-filled 2p orbital, oriented normal to the graphene plane, forms a *pi* bond with a nn C atom and thus gets delocalized. It is the latter – in a TB-depiction of the underlying honecomb lattice – which leads to electron bands that is at the core of all electronic properties.

5. The intrinsic half-filled character of the π orbital is at the root cause of a completely filled valence band and a totally empty conduction band.

6. The conduction and valence bands touch each other at 6 symmetric points in the **k**-space (in consonance with 6 sites in the hexagonal lattice, in real space) of which two are special (other 4 being mirror images): the K and K′ points in the Brillouin zone. At these 6 points the 'band gap' between the conduction and valence bands vanishes.

7. The K and K′ points are symmetrically situated with regard to the zero of what is usually referred to as the Fermi level.Near the K and K′ points (hence, in the vicinity of the Fermi level, where all the action is!),the energy dispersion is linear in the wave vector **q**, thus endowing the electrons with zero-mass fermion attribute.

8. The symmetric K and K′ states are like the two states of a Dirac spinor, sometimes called a pseudo-spin, in the context of graphene [9]. Combined with the two other possibilities of conduction ('particle') and valence ('hole') states one arrives at a remarkable analogy with the 4-component relativistic Dirac theory of massless excitations. Here, we prefer to reserve the nomenclature 'pseudo-spin' for denoting the particle-hole states. It should be recognized though that the fermionic excitations in graphene travel with not the speed of light but with a velocity that is three hundred times smaller.

The extraordinary resemblance between the graphene physics with 2+1-dimensional Dirac theory for massless electrons makes it possible to apply many of the ideas of relativistic quantum mechanics at the level of laboratory experiments.

In conclusion, the extraordinary resemblance between the graphene physics with 2+1-dimensional Dirac theory for massless electrons makes it possible to apply many of the ideas of relativistic quantum mechanics at the level of laboratory experiments. Besides, the two-dimensional crystalline structure of graphene allows for novel applications to quantum Hall effectand nanoscopic devices.

Acknowledgement

I am grateful to the Indian National Science Academy for its support through their Senior Scientistscheme and to the Bose Institute, Kolkata for affiliation. This article resulted from a series of lectures delivered at the Indian Institute of Science Education and Research (IISER), Mohali. I am thankful to IISER, Mohali and in particular, to Dr. Goutam Sheet for their kind hospitality. Thanks are also due to Ms. AnshuSirohi for her help with the figures.

Suggested Reading

[1] G W Semenoff, Condensed-Matter Simulation of a Three-Dimensional Anomaly, *Physical Review Letters*, Vol.53, p.2449, 1984.

[2] A H Castro Neto, F Guinea, N M R Peres, K S Novoselov and A K Geim, The Electronic Properties of Graphene, *Reviews of Modern Physics*, Vol.81, p.109, 2009.

[3] G Baskaran, Physics of Quanta and Quantum Fields in Graphene, in, *Graphene: Synthesis, Properties and Phenomena*, First Edition, Edited by C. N. R Rao and A K Sood, Wiley-VCH Verlag GmbH & Co., 2013.

[4] *Graphene and Its Fascinating Attributes*, eds., S. K. Pati, T. Enoki and C. N. R. Rao, World Scientific, Singapore, 2011.

[5] *Graphene: Synthesis, Properties and Phenomena*, First Edition, Edited by C. N. R. Rao and A. K. Sood, Wiley-VCH Verlag GmbH & Co., 2013.

[6] R M Saito, G Dresselhaus and M S Dresselhaus, *Physical Properties of Carbon Nanotubes*, Imperial College Press, London, 1998.

[7] H W Kroto, J R Heath, S C O'Brien, R F Curl and R E Smalley, *Nature* (London), Vol.318, p.162, 1985.

[8] A K Geim and K S Novoselov, *Nature Mater.*, Vol.6, p.183, 2007.

[9] M M Desmukh and V Singh, Graphene – An Exciting Two-Dimensional Material for Science and Technology, *Resonance*, Vol. March, p.238, 2011.

[10] S Potnis, From Carbon to Bucky Paper, *Resonance*, Vol. March, p.257, 2017.

[11] P W Atkins, *Physical Chemistry*, ELBS with Oxford University Press, London, Chapters 13 and 14, 1994.

[12] G N Lewis, apart from the valence-bond theory, also pioneered the electronic theory of acids and bases. Ironically, Lewis, whose middle name is Newton, coined the phrase 'photon' for light quantum in 1926 – a notion which completely altered the Newtonian view of light!

[13] C Kittel,*Introduction to Solid State Physics*, 6th edition, John Wiley and Sons, N. Y., 1986.

[14] E Merzbacher, *Quantum Mechanics*, John Wiley and Sons, N. Y., 1970.

[15] L Pauling, *The Nature of the Chemical Bond*, Cornell University Press, U. S. A., 1960.

[16] S Dattagupta, Quantum Phase and Its Measurable Attributes a laAharonov-Bohm Effect, *Resonance*, September Issue, Sec. 3.1, 2018.

[17] For a historical perspective, see Arvind, K Dorai, S Chaturvedi and N Mukunda, The Development of Quantum Mechanics, *Resonance*, October, 2018.

[18] J J Sakurai, *Advanced Quantum Mechanics*, Addison-Wesley, Reading, Massachusetts, 1967.

Address for Correspondence
Sushanta Dattagupta
Uniworld City
Heights Tower 6, Flat 002
New Town (Action Area III)
Rajarhat, Kolkata 700 156
Email:sushantad@gmail.com